Ni^{3+} doped cobalt-nickel layered double hydroxides as high performance electrode material for supercapacitors

Hongmei Sun,[a,b] Yixing Ye,[a] Zhenfei Tian,[a] Shouliang Wu,[a] Jun Liu,[a]* and Changhao Liang [a,b]

[a]Key Laboratory of Materials Physics and Anhui Key Laboratory of Nanomaterials and Nanotechnology, Institute of Solid State Physics, Hefei Institutes of Physical Science, Chinese Academy of Sciences, Hefei 230031, China.

[b]Department of Materials Science and Engineering, University of Science and Technology of China, Hefei 230026,China.

*Corresponding author. E-mail: jliu@issp.ac.cn

Abstract

Co-Ni layered double hydroxides (LDHs), as promising supercapacitor electrode materials with high specific capacity, have suffered poor rate property and cycle stability. By doping and topochemical oxidation of Ni ions is considered as efficivent rout to overcome these drawbacks. In this work, Ni^{3+} doped cobalt-nickel layered double hydroxides (Co-Ni-LDHs) were synthesized by pluse laser ablation of Ni taget in $CoCl_2$ aqeous solution. The existence of Ni^{3+} ions doped in Co-Ni-LDHs decline the conductive resistance, and increase the mobility of surface charge and transfer rate of electrolyte. As a results, the Ni^{3+} doped Co-Ni-LDHs display a maximum specific capacitance of 2275 F/g and 1450 F/g at the current density of 1 A/g and 20 A/g, respectivly, indicating a high rate specific capacitance. Moreover, the capacitance retention is to be 80% after 1800 cycles at the current density of 6 A/g, manifesting good cycling stability of Ni^{3+} doped Co-Ni-LDHs.

Keywords: laser ablation in liquids, Ni^{3+} doped cobalt-nickel layered double hydroxides, supercapacitors materials, excellent rate capability, good cycling stability

1.Introduction

Transition metal-based layered double hydroxides materials (LDHs) are considered as one of the most promising materials for pseudocapacitor, owing to the low cost, environmental friendliness and high theoretical capacitance. [1] [2] [3] Compared to monometallic hydroxide, LDHs present two kinds of metal inserted in the host layer, which could provide richer redox reactions and offer an effective way for achieving improved electrochemical performance. [4] [5]However, the poor rate capacitance and cycle stability due to the severe large volume expansion and the poor conductivity limit the practical applications of LDHs structure for supercapacitors materials. To overcome these disadvantages, substantial efforts are focused on the efficient incorporation of high conductive materials such as graphene, CNT, conductive polymers into the LDHs composites to improve the conductivity. [6] [7] For example, Huang [8] et al. fabricated

CoNiAl-LDH nanosheets attached on sandwich-like reduced graphene oxide (RGO) with 1866 F/g at the current density of 1 A/g while maintaining 1360F/g at the current density of 10 A/g. Another strategy is to design hierarchical or porous structure with high surface area grown on the current collector (nickel foam[9], conductive textile substrate[10]) to buffer the volume expansion.[11] [12] But the low material loading masses are not suitable for application.

Recently, engineering M^{3+} in LDHs phase has emerged as an effective approach for solving this problems. The M^{3+}(M= Ni, Co) species of LDHs play a key role in the efficiency of the active metal sites as well as controlling electron-transfer rate. [13] [14] [15]Wang[16] etched Al in Ni-Co-Al LDH by NaOH to enable the partial conversion of Co^{2+} to Co^{3+} with enhanced conductivity. Compared to Ni-Co-Al LDH, Ni-Co-Al LDHs after NaOH treatment display the lower resistance which lead to faster electrode kinetics. Moreover, theoretical studies[17] has demonstrated the spin-up states of Ni^{3+} in monolayer NiTi-LDH (0.9 nm) can improve density of states values around the Fermi level, demonstrating a half-metallic characteristic to improve carrier mobility and electrical conductivity. Therefore, M^{3+} in LDHs are desirable to improve electrochemical performance. [18] [19] Although good results were obtained by doping M^{3+}, special chemical treatments to the precursory compounds are generally needed to induce the transformation from M^{2+} to M^{3+}. For example, Co^{3+} doped layered double hydroxides were synthesized through a topochemical oxidative reaction employing bromine[20] (Br_2), O_2 [15], NO_3^- ions [8] as an oxidizing agent, or chemical etching of Al in Ni-Co-Al LDH by NaOH [9] [18]. Therefore, it is still need to explore a simple and green strategy method to synthesize M^{3+} doped layered double hydroxides materials.

Laser ablation in liquids (LAL) technique has been demonstrated a novel strategy to fabricate nanomaterials with desired size, structures and components.[23-25] Also, it's an effective rout to achieving doping ions into hydroxides. For example, our group has fabricated Mn-doped $Ni(OH)_2$ nanosheets,[26] Co-doped $Ni(OH)_2$ [27] by laser ablation Mn or Co target in $NiCl_2$ aqueous solution. In this work, by laser ablation of Ni target in $CoCl_2$ aqueous solution, doping and topochemical oxidation of Ni^{3+} ions were simultaneously accomplished in one step. We

successfully fabricate the Ni^{3+} doped cobalt-nickel layered double hydroxides (Co-Ni-LDHs). Moreover, as-synthesized Ni^{3+} doped Co-Ni-LDHs used as electrode materials for supercapacitors display high rate specific capacitance and excellent cycling stability.(特点和结果)

2.Experimental section

2.1 LAL assisted formation of Co-Ni-LDHs

As shown in Figure S1, firstly, a nickel target (99.99% in purity) is fixed in a vessel filled with 18 mL 0.01 M $CoCl_2$ solution, and ablated for 30 min by a Nd:YAG laser with wavelength of 1064 nm, pulse duration of 10 ns and per pulse laser energy of 120 mJ. The obtained colloidal solution was aged for 15 h. The precipitate is the final products and subsequently washed with ethanol and deionized water alternately for three times for characterization and application in supercapacitors.

2.2 Characterization of Co-Ni-LDHs

Scanning electron microscopy (SEM) system (Sirion 200 FEG) was used to observe the morphology of the Co-Ni-LDHs nanostructures. Energy dispersive X-ray spectrometry (EDX) was used to determine the element content. A transmission electron microscopy (TEM) system (JEOL, JEM-2010) with a 200 KV acceleration voltage was used to obtain the structural information of the products and element distribution. X-ray diffraction (XRD) analysis of the collected powder products was performed by using a Philips X'Pert system with Cu-Kα radiated (λ = 1.5419 Å). The surface chemical states were analyzed by X-ray photoelectron spectroscopy (XPS; Thermo ESCACLB 250). The surface area and porosity of the samples were measured using an Omnisorp 100CX Analyzer (Beckman Coulter, Inc., USA).

2.3 Supercapacitors performance of Co-Ni-LDHs

The as-prepared samples were used as electro-active materials for supercapacitors. The electrochemical performances of electrodes were evaluated on a Zahner electrochemical workstation (Germany) at room temperature and measured in 3 M KOH electrolyte. The working electrode was prepared by dispersing the samples into N-methyl pyrrolidone and mixed with polyvinylidene fluoride and acetylene black in a mass ratio of 8:1:1 and then painted on Ni foam. The mass loading of the powders on the nickel foam (1 cm×1 cm) was determined by subtracting the weight before deposition from that after deposition and calculated to be around 3 mg/cm^2. The test system is a standard three-electrode configuration, including an Ag/AgCl electrode as a reference electrode and a platinum foil as the counter electrode. The specific capacitance of the electrode could be calculated according to equation 1. Where C_{SP} is the specific capacitance (F/g), I is the current density (A), Δt is the discharge time (s) and ΔV is the potential window (V), m is the mass of the active materials (g), respectively.

3. Results and discussion

3.1 Morphological and structural characterization

Figure 1 (a) XRD pattern of Co-Ni-LDHs, (b) N_2 adsorption desorption isotherms and pore-size-distribution curves of Co-Ni-LDHs, (c) SEM image of Co-Ni-LDHs, (d) TEM image of Co-Ni-LDHs, (e) TEM image and the corresponding SAED pattern of individual Co-Ni-LDHs nanosheets, (f) EDX elemental mapping images of Co-Ni-LDHs.

Figure 1a presents the XRD pattern of as-synthesized Co-Ni-LDHs. The two prominent low-angle diffraction peaks located at 11.21° and 22.69° are assigned to (003) and (006) lattice planes of the hydrotalcite-like LDHs phase, which are similar to the standard XRD peaks for α-$Co(OH)_2$ phase (JCPDS No. 42-1467).[28] In addition, the (00h) reflections present sharp,

symmetric and high diffraction intensity, suggesting that the synthesized structure is well crystallized with a regular interlayer and the preferential orientation growth along <00h> zone axis. Corresponding SEM and TEM image of Co-Ni-LDHs (Figure 1c, d) show typical morphology of aggregated nanosheets that interconnect with each other to form a porous structure. Calculated by the Barrett-Joyner-Halenda (BJH) model (Figure 1b), the specific surface area and pore diameter is of 201.9 m^2/g and 11.3 nm, respectively, which is much larger than that of $Ni(OH)_2$ nanosheets (114 m^2/g)[26] and floss-like Ni-Co binary hydroxides (106.5 m^2/g) [27]. Such large specific surface area and nanosheets-based porous structures allow high access of electrolyte to the integrated nanosheets, which is crucial for the reduction of the interface contact resistance between the electrodes and electrolyte. [28] TEM image of several separated nanosheets (Figure 1e) reveals a hexagonal shape of Co-Ni-LDHs, and the corresponding SAED pattern (inset in Figure 1e) presents perfect hexagonal diffraction spots well matched with d-spacing of (110) lattice plane, indexed as the two-dimensional in-plane reflections. EDS spectrum (Figure S2 in ESI†) of products demonstrates that the element ratio of Co and Ni is to be 0.55:0.45, thus it can be marked as $Co_{0.55}Ni_{0.45}$-LDHs. Also, the EDS elemental mapping images (Figure 1f) verify that all elements (Co, Ni and O) are uniformly distributed in $Co_{0.55}Ni_{0.45}$-LDHs.

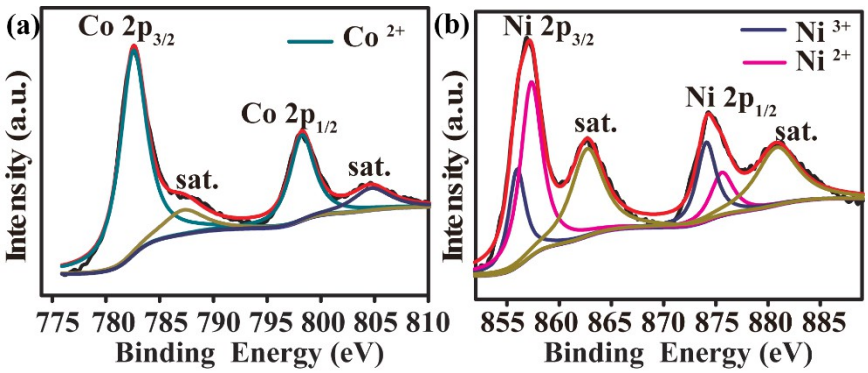

Figure 2 XPS spectra of $Co_{0.55}Ni_{0.45}$-LDHs (a) Co 2p, (b) Ni 2p.

XPS spectra is used to analyze the valence states of $Co_{0.55}Ni_{0.45}$-LDHs. The C 1s peak at 284.8 eV 用于分析其它元素的价键。$Co_{0.55}Ni_{0.45}$-LDHs 的全谱 XPS 曲线 (Figure S3a) present sharp photoelectron peaks of Co, Ni, O and C elements. Figure S3b shows the fine XPS spectrum of O 1s, the peak located at 531.1 eV is related to hydroxyl ions.[35] In the Co 2p region

(Figure 2a), one pair of binding energies located at 782.5 eV and 798.5 eV coincide with Co^{2+}.[29] [30] While in the Ni 2p region (Figure 2b), two typical Ni^{2+} $2p_{3/2}$ and Ni^{3+} $2p_{3/2}$ peaks centered at 856.3eV and 855.9 eV are co-existed in the $Co_{0.55}Ni_{0.45}$-LDHs.[30] It means that Ni^{3+} ions were doped in $Co_{0.55}Ni_{0.45}$-LDHs, which is ascribed to the unique LAL reaction process described as follows. As pulse laser irradiating on the interface between Ni target and liquid, a plasma plume with high temperature, high pressure environment, containing Ni species (including atoms, ions, and radicals) is produced. The Ni species in the plasma plume continuously reacts with oxygen dissolved in solution or water, parts of Ni ions can be easily oxidized to Ni^{3+} ions. Simultaneously, the Ni species and Co^{2+} in the solution continuously reacts with the ions and radicals such as OH^- to form Ni^{3+} doped $Co_{0.55}Ni_{0.45}$-LDHs.[31]

3.2. Supercapacitors performance of $Co_{0.55}Ni_{0.45}$-LDHs

$Co_{0.55}Ni_{0.45}$-LDHs are used as electrode materials for supercapacitors, electrochemical performance are investigated by cyclic voltammetry (CV), galvanostatic charge-discharge measurements and electrochemical impedance spectroscopy (EIS). CV curves of $Co_{0.55}Ni_{0.45}$-LDHs (Figure 3a) at the first test cycle present obvious redox peaks, revealing pseudocapacitive characteristics, which differ from the nearly rectangular CV shapes for conventional EDLCs.[32] The reactions involved could be interpreted as follows: [33]

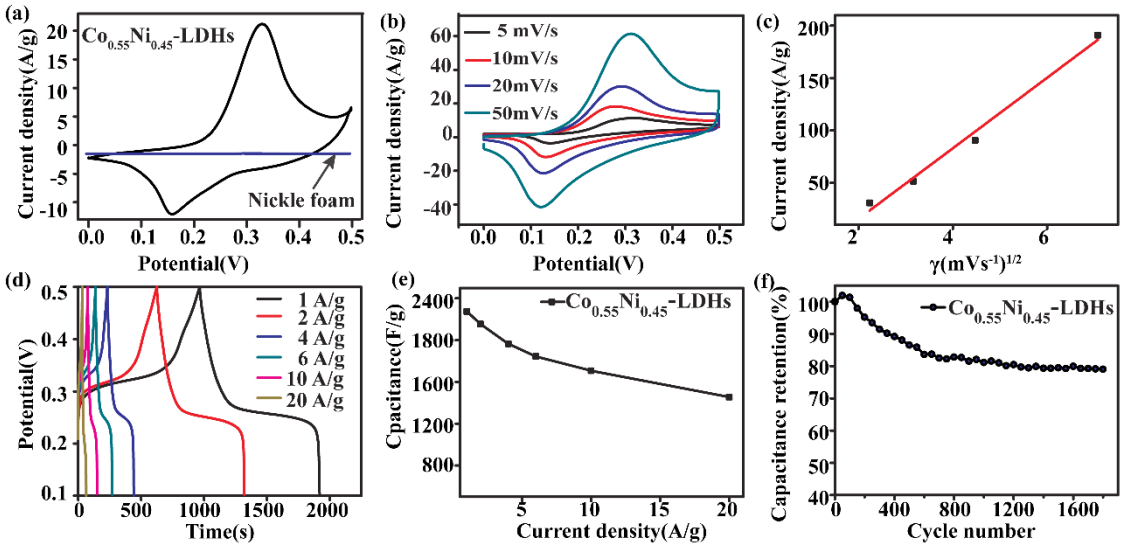

Figure 3 (a) CV curves of $Co_{0.55}Ni_{0.45}$-LDHs at scan rate of 5 mV/s, (b) CV curve of $Co_{0.55}Ni_{0.45}$-LDHs at various scan rates, (c) The linear relationship of $Co_{0.55}Ni_{0.45}$-LDHs between the oxidation peak currents and the square root of scan rates, (d) Galvanostatic charge-discharge curves of $Co_{0.55}Ni_{0.45}$-LDHs at 1, 2, 4, 6, 10, and 20 A/g, (e) The specific capacitance of the $Co_{0.55}Ni_{0.45}$-LDHs at 1, 2, 4, 6, 10, and 20 A/g, (f) Cycling performance at a scan rate of 6 A/g of $Co_{0.55}Ni_{0.45}$-LDHs

In addition, CV curves within the potential window of 0.0-0.5 V (vs. Ag/AgCl) at various scan rates from 5 to 50 mV/s is evaluated and shown in Figure 3b. With the rising of scan rate, the currents increase and the potentials of redox peaks shift to a more negative or positive position. This phenomenon is mainly due to the fact that the increasing of scan rate would cause the rising in the internal diffusion resistance within the pseudoactive materials.[34] Furthermore, even at high scan rate of 50 mV/s, the shape of CV curve does not significantly distort, implying the nature of fast electron transport. Here, the good linear relationship between the oxidation peak currents and the square root of scan rates (Figure 3c) confirms that the electrode reaction of Co/Ni-LDHs is diffusion controlled.[35]

In order to further evaluate the rate capacity and cycling stability of the prepared $Co_{0.55}Ni_{0.45}$-LDHs, galvanostatic charge-discharge (GCD) measurements were conducted. Figure 3d shows the GCD of the $Co_{0.55}Ni_{0.45}$-LDHs at different current densities from 1 A/g to 20 A/g in a voltage range of 0.1-0.5 V. The well-defined charge and discharge plateaus in all curves demonstrate

the existence of redox reaction, confirming the foregoing CV results. The specific capacitance of the $Co_{0.55}Ni_{0.45}$-LDHs (Figure 3e) composite is calculated to be 2275, 2153, 1965, 1845, 1708 and 1450 F/g at the current discharge of 1, 2, 4, 6, 10, and 20 A/g according to equation (1). The specific capacitance retention of $Co_{0.55}Ni_{0.45}$-LDHs at different current densities is displayed in Figure S4. The high capacity retention of 64% are achieved for $Co_{0.55}Ni_{0.45}$-LDHs when the current density is increased from 1A/g to 20 A/g, displaying high rate capability. Figure 3f displays the cyclic performance of the obtained $Co_{0.55}Ni_{0.45}$-LDHs composite at a current density of 6 A/g. It can be seen that the specific capacitance shows a gradual decrease at first, and it is nearly constant after 800 cycles. After 1800 cycles, there is still 80% capacitance retention for $Co_{0.55}Ni_{0.45}$-LDHs electrode, indicating a good cycling stability.

Table 1 Comparison of various relative results of Co-Ni-LDHs.

Material	Specific capacitance (F/g)	Current density (A/g)	Reference
$Co_{0.55}Ni_{0.45}$-LDHs	1708	10	This work
	1450	20	This work
Ni^{3+} doped NiTi-LDHs	1500	20	[17]
RGO@CoNiAl-LDHs	1360	10	8
α phase Ni-Co bimetallic hydroxides	1350	20	33
floss-like Ni-Co binary hydroxides	594	10	27
$Ni(OH)_2$ hexagonal platelets	628	10	[34b]
CoNiAl-LDHs/GO	618	20	[7]

In comparison with the previously reported results(Table 1), including RGO@CoNiAl-LDH, [8] floss-like Ni-Co binary hydroxides[27] and α-phase Ni-Co bimetallic hydroxides[33], here synthesized $Co_{0.55}Ni_{0.45}$-LDHs exhibit better specific capacitance. The achieved higher specific capacitance, excellent rate capability and the long cycle life may be understood as following issues: (a) The Ni^{3+} promote electron transportation to reduce the conductivity of $Co_{0.55}Ni_{0.45}$-LDHs; [17] (b) The high specific surface area and porous structure of $Co_{0.55}Ni_{0.45}$-LDHs could shorten the diffusion distance between the electrolyte and electrodes, which can promote deep ions diffusion in electrochemical reaction; [29] [36] (c) The uniform distribution of Ni is a key factor

to ensure the electron transfer, which can effectively optimize the electrical conductivity and durability of the electrode materials; [19]

Conclusions

In summary, Ni^{3+} doped $Co_{0.55}Ni_{0.45}$-LDHs were prepared by liquid-phase laser ablation method. Detailed characterization reveal Ni^{3+} doped $Co_{0.55}Ni_{0.45}$-LDHs hexagonal sheet-like shape, high specific surface area, porous structures and uniform distribution of Co, Ni elements. As electrode materials for supercapacitors, $Co_{0.55}Ni_{0.45}$-LDHs yields a maximum specific capacitance of 2275 F/g at 1 A/g, and 1450 F/g at high current density of 20 A/g, which indicate a high rate capacity. Furthermore, $Co_{0.55}Ni_{0.45}$-LDHs present 80% capacitance retention after 1800 cycles at 6 A/g, meaning long cycle life for energy storage applications. Overall, this work provide a novel and efficient strategy in engineering M^{3+} in LDHs phase, and confirmed that is an effective approach for improving their supercapacitor performance for practical energy storage devices.

Acknowledgements

This work was financially supported by the National Basic Research Program of China (2014CB931704), the National Natural Science Foundation of China (NSFC, No. 51371166, 51401206, 51571186, 11674321, 11504375) and the CAS/SAFEA International Partnership Program for Creative Research Teams).

1. Zhao, Y.; Liu, J.; Hu, Y.; Cheng, H.; Hu, C.; Jiang, C.; Jiang, L.; Cao, A.; Qu, L., Highly Compression-Tolerant Supercapacitor Based on Polypyrrole-mediated Graphene Foam Electrodes. *Adv Mater* **2013,** *25* (4), 591-595.
2. Pu, J.; Tong, Y.; Wang, S. B.; Sheng, E. H.; Wang, Z. H., Nickel-cobalt hydroxide nanosheets arrays on Ni foam for pseudocapacitor applications. *J Power Sources* **2014,** *250*, 250-256.
3. (a) Chen, Z.; Qin, Y. C.; Weng, D.; Xiao, Q. F.; Peng, Y. T.; Wang, X. L.; Li, H. X.; Wei, F.; Lu, Y. F., Design and Synthesis of Hierarchical Nanowire Composites for Electrochemical Energy Storage. *Adv Funct Mater* **2009,** *19* (21), 3420-3426; (b) Birjega, R.; Matei, A.; Filipescu, M.; Stokker-Cheregi, F.; Luculescu, C.; Colceag, D.; Zavoianu, R.; Pavel, O. D.; Dinescu, M., The investigation of Ni-Al and Co-Al based layered double hydroxides and their derived mixed oxides thin films deposited by pulsed laser deposition. *Applied Surface Science* **2013,** *278*, 122-126.
4. Salunkhe, R. R.; Bastakoti, B. P.; Hsu, C.-T.; Suzuki, N.; Kim, J. H.; Dou, S. X.; Hu, C.-C.; Yamauchi, Y., Direct Growth of Cobalt Hydroxide Rods on Nickel Foam and Its Application for Energy Storage. *Chem-Eur J* **2014,** *20* (11), 3084-3088.
5. Ma, W.; Wang, L.; Xue, J.; Cui, H., Ultra-large scale synthesis of Co–Ni layered double hydroxides monolayer nanosheets by a solvent-free bottom-up strategy. *J Alloy Compd* **2016,** *662*, 315-319.
6. Wang, L.; Wang, D.; Dong, X. Y.; Zhang, Z. J.; Pei, X. F.; Chen, X. J.; Chen, B.; Jin, J., Layered assembly of graphene oxide and Co-Al layered double hydroxide nanosheets as electrode materials for supercapacitors. *Chem Commun* **2011,** *47* (12), 3556-3558.
7. Fang, J.; Li, M.; Li, Q.; Zhang, W.; Shou, Q.; Liu, F.; Zhang, X.; Cheng, J., Microwave-assisted synthesis of CoAl-layered double hydroxide/graphene oxide composite and its application in supercapacitors. *Electrochim Acta* **2012,** *85*, 248-255.
8. Huang, P.; Cao, C.; Sun, Y.; Yang, S.; Wei, F.; Song, W., One-pot synthesis of sandwich-like reduced graphene oxide@CoNiAl layered double hydroxide with excellent pseudocapacitive properties. *J Mater Chem A* **2015,** *3* (20), 10858-10863.
9. Abushrenta, N.; Wu, X.; Wang, J.; Liu, J.; Sun, X., Hierarchical Co-based Porous Layered Double Hydroxide Arrays Derived via Alkali Etching for High-performance Supercapacitors. *Sci Rep-Uk* **2015,** *5*.
10. Nagaraju, G.; Raju, G. S. R.; Ko, Y. H.; Yu, J. S., Hierarchical Ni-Co layered double hydroxide nanosheets entrapped on conductive textile fibers: a cost-effective and flexible electrode for high-performance pseudocapacitors. *Nanoscale* **2016,** *8* (2), 812-825.
11. Zhang, Q.; Chen, H.; Wang, J.; Xu, D.; Li, X.; Yang, Y.; Zhang, K., Growth of Hierarchical 3D Mesoporous NiSix/NiCo2O4 Core/Shell Heterostructures on Nickel Foam for Lithium-Ion Batteries. *Chemsuschem* **2014,** *7* (8), 2325-2334.
12. Cheng, J. P.; Fang, J. H.; Li, M.; Zhang, W. F.; Liu, F.; Zhang, X. B., Enhanced electrochemical performance of CoAl-layered double hydroxide nanosheet arrays coated by platinum films. *Electrochim Acta* **2013,** *114*, 68-75.
13. Gu, F.; Cheng, X.; Wang, S. F.; Wang, X.; Lee, P. S., Oxidative Intercalation for Monometallic Ni2+-Ni3+ Layered Double Hydroxide and Enhanced Capacitance in Exfoliated Nanosheets. *Small* **2015,** *11* (17), 2044-2050.
14. (a) Vialat, P.; Rabu, P.; Mousty, C.; Leroux, F., Insight of an easy topochemical oxidative reaction in obtaining high performance electrochemical capacitor based on (CoCoIII)-Co-II monometallic cobalt Layered Double Hydroxide. *J Power Sources* **2015,** *293*, 1-10; (b) Xie, J.; Sun, X.; Zhang, N.; Xu, K.; Zhou, M.; Xie, Y., Layer-by-layer β-Ni(OH)2/graphene nanohybrids for ultraflexible all-solid-state thin-film supercapacitors with high electrochemical performance. *Nano Energy* **2013,** *2* (1), 65-74.
15. Vialat, P.; Mousty, C.; Taviot-Gueho, C.; Renaudin, G.; Martinez, H.; Dupin, J.-C.; Elkaim, E.; Leroux, F., High-Performing Monometallic Cobalt Layered Double Hydroxide Supercapacitor with Defined Local Structure. *Adv Funct Mater* **2014,** *24* (30), 4831-4842.
16. Wang, X.; Yan, C.; Sumboja, A.; Yan, J.; Lee, P. S., Achieving High Rate Performance in Layered Hydroxide Supercapacitor Electrodes. *Adv Energy Mater* **2014,** *4* (6), 1301240.
17. Zhao, Y.; Wang, Q.; Bian, T.; Yu, H.; Fan, H.; Zhou, C.; Wu, L.-Z.; Tung, C.-H.; O'Hare, D.; Zhang, T., Ni3+ doped monolayer layered double hydroxide nanosheets as efficient electrodes for supercapacitors. *Nanoscale* **2015,** *7* (16), 7168-7173.
18. Wu, X. L.; Jiang, L. L.; Long, C. L.; Wei, T.; Fan, Z. J., Dual Support System Ensuring Porous Co-Al Hydroxide Nanosheets with Ultrahigh Rate Performance and High Energy Density for Supercapacitors. *Adv Funct Mater* **2015,** *25* (11), 1648-1655.
19. Chen, H.; Hu, L. F.; Chen, M.; Yan, Y.; Wu, L. M., Nickel- Cobalt Layered Double Hydroxide Nanosheets for High- performance Supercapacitor Electrode Materials. *Adv Funct Mater* **2014,** *24* (7), 934-942.
20. Liang, J.; Ma, R.; Iyi, N.; Ebina, Y.; Takada, K.; Sasaki, T., Topochemical Synthesis, Anion Exchange, and Exfoliation of Co−Ni Layered Double Hydroxides: A Route to Positively Charged Co−Ni Hydroxide Nanosheets with Tunable Composition. *Chem Mater* **2010,** *22* (2), 371-378.
21. Zhang, H. M.; Liu, J.; Ye, Y. X.; Tian, Z. F.; Liang, C. H., Synthesis of Mn-doped alpha-Ni(OH)(2) nanosheets assisted by liquid-phase laser ablation and their electrochemical properties. *Phys Chem Chem Phys* **2013,** *15* (15), 5684-5690.
22. Liu, J.; Liang, C. H.; Zhang, H. M.; Tian, Z. F.; Zhang, S. Y., General Strategy for Doping Impurities (Ge, Si, Mn, Sn, Ti) in Hematite Nanocrystals. *J Phys Chem C* **2012,** *116* (8), 4986-4992.
23. Liu, J.; Liang, C.; Xu, G.; Tian, Z.; Shao, G.; Zhang, L., Ge-doped hematite nanosheets with tunable doping level, structure and improved photoelectrochemical performance. *Nano Energy* **2013,** *2* (3), 328-336.
24. Tian, Z.; Liang, C.; Liu, J.; Zhang, H.; Zhang, L., Reactive and photocatalytic degradation of various water contaminants by laser ablation-derived SnOx nanoparticles in liquid. *J Mater Chem* **2011,** *21* (45), 18242.
25. Zhaoping Liu, Renzhi Ma, Minoru Osada, Kazunori Takada, and Takayoshi Sasak, Selective and Controlled Synthesis of α- and β-CobaltHydroxides in Highly Developed Hexagonal Platelets. **2005**.
26. Sun, W. P.; Rui, X. H.; Ulaganathan, M.; Madhavi, S.; Yan, Q. Y., Few-layered Ni(OH)(2) nanosheets for high-performance supercapacitors. *J Power Sources* **2015,** *295*, 323-328.
27. Tang, Y.; Liu, Y.; Guo, W.; Yu, S.; Gao, F., Floss-like Ni–Co binary hydroxides assembled by whisker-like nanowires for high-performance supercapacitor. *Ionics* **2014,** *21* (6), 1655-1663.
28. Chen, J.-C.; Hsu, C.-T.; Hu, C.-C., Superior capacitive performances of binary nickel-cobalt hydroxide nanonetwork prepared by cathodic deposition. *J Power Sources* **2014,** *253*, 205-213.
29. Quan, W.; Tang, Z. L.; Hong, Y.; Wang, S. T.; Zhang, Z. T., Hydroxyl compensation effects on the cycle stability of Nickel-Cobalt layered double hydroxides synthesized via solvothermal method. *Electrochim Acta* **2015,** *182*, 445-451.

30. Cai, X.; Shen, X.; Ma, L.; Ji, Z.; Xu, C.; Yuan, A., Solvothermal synthesis of NiCo-layered double hydroxide nanosheets decorated on RGO sheets for high performance supercapacitor. *Chemical Engineering Journal* **2015,** *268*, 251-259.
31. Liu, X. Y.; Gao, Y. Q.; Yang, G. W., A flexible, transparent and super-long-life supercapacitor based on ultrafine Co3O4 nanocrystal electrodes. *Nanoscale* **2016,** *8* (7), 4227-4235.
32. Simon, P.; Gogotsi, Y., Materials for electrochemical capacitors. *Nat Mater* **2008,** *7* (11), 845-854.
33. Xia, D.; Chen, H.; Jiang, J.; Zhang, L.; Zhao, Y.; Guo, D.; Yu, J., Facilely synthesized α phase nickel–cobalt bimetallic hydroxides: Tuning the composition for high pseudocapacitance. *Electrochim Acta* **2015,** *156*, 108-114.
34. (a) Li, J.; Yang, M.; Wei, J.; Zhou, Z., Preparation and electrochemical performances of doughnut-like Ni(OH)(2)-Co(OH)(2) composites as pseudocapacitor materials. *Nanoscale* **2012,** *4* (15), 4498-503; (b) Li, L. J.; Xu, J.; Lei, J. L.; Zhang, J.; McLarnon, F.; Wei, Z. D.; Li, N. B.; Pan, F. S., A one-step, cost-effective green method to in situ fabricate Ni(OH)(2) hexagonal platelets on Ni foam as binder-free supercapacitor electrode materials. *J Mater Chem A* **2015,** *3* (5), 1953-1960.
35. Li, Y. W.; Yao, J. H.; Liu, C. J.; Zhao, W. M.; Deng, W. X.; Zhong, S. K., Effect of interlayer anions on the electrochemical performance of Al-substituted α-type nickel hydroxide electrodes. *Int J Hydrogen Energ* **2010,** *35* (6), 2539-2545.
36. Min, S. D.; Zhao, C. J.; Zhang, Z. M.; Chen, G. R.; Qian, X. Z.; Guo, Z. P., Synthesis of Ni(OH)(2)/RGO pseudocomposite on nickel foam for supercapacitors with superior performance. *J Mater Chem A* **2015,** *3* (7), 3641-3650.